construct (*20*). Mutagenesis, sequencing, and recloning was as described (*5*). Reporters were introduced into *Saccharomyces cerevisiae* strains BSY17 (*7*), BSY398 [*MATα, CAN1, his4, leu2, trp1, ura3, snr6::LEU2*, pBS521 (2 μm, WT-U6, TRP1)], or BSY399 [*MATα, CAN1, his4, leu2, trp1, ura3, snr6::LEU2*, pBS605 (2 μm, U6-44/46, TRP1)].

22. β-galactosidase assays were as described [L. Guarente and M. Ptashne, *ibid.* **78**, 2199 (1981)] or conducted with a modification of the original protocol in which the chloroform-SDS mixture was replaced by 200 μl of ether. In the latter case, ether was evaporated before the assay. Assays were done in duplicate and data represent average values. The variation between duplicate samples was at most 25%.
23. RNA extraction and primer extension were as described (*5*). The RB27 primer complementary to intron sequences downstream of the 5′ splice was used to map the cleavage site on lariat molecules (*8*). Because the efficiency of the second splicing step is different for RNAs cleaved at the normal or aberrant splice site, it is not possible to compare quantitatively the analyses by primer extension and enzymatic assay.
24. J. J. SantaLucia, R. Kierzek, D. H. Turner, *Biochemistry* **30**, 8242 (1991).
25. Analysis of 74 different yeast introns indicate that the yeast consensus sequence at the 5′ splice site is rr/GuauGuwx, in which uppercase letters represent completely conserved nucleotides, r: purine, w: A or U, x: any nucleotide and /: the 5′ splice junction. Thus, there seems to be no selection after position 6 in the intron for pairing with nucleotides upstream of position 47 in U6 snRNA. However, a U that can not base pair with U1 snRNA but can with U6 snRNA is conserved at position 4. In human, the 5′ splice site consensus is kag/Gtragtr (symbols as above with k being A or C) [R. M. Stephens and T. D. Schneider, *J. Mol. Biol.* **228**, 1124 (1992)]. G at position 5 of the intron is the third most highly conserved nucleotide in that consensus. There could be pairing between U6 position 46 to 48 and nucleotides 5 to 7 of 5′ splice sites.
26. A similar strategy with a different reporter gene and similar results are reported by C. Lesser and C. Guthrie [*Science* **262**, 1982 (1993)].
27. B. Datta and A. M. Weiner, *Nature* **352**, 821 (1991); J. Wu and J. L. Manley, *ibid.*, p. 818.
28. H. D. Madhani and C. Guthrie, *Cell* **71**, 803 (1992).
29. Analysis of constructs with an A at intron position 5 and various substitutions in the last two bases of the upstream exon indicate that the level and location of the aberrant cleavages' events are consistent with base pairing of U5 snRNA with nucleotides preceding the cleaved phosphodiester bond (*18*).
30. We thank D. Brow for plasmids and yeast strains, P. Legrain for suggestion on the β-galactosidase assay, C. Lesser, C. Guthrie, E. Sontheimer, and J. Steitz for exchange of information before publication, and the EMBL services for their help. We are grateful to K. Bohmann, C. Dingwall, E. Izaurralde, S. Gunderson, J. Lewis, Z. Lygerou, I. Mattaj, F. Mauxion, and K. Weis for their thoughtful discussions and comments on the manuscript. We thank I. Mattaj and EMBL for support.

12 August 1993; accepted 23 November 1993

Connexin Mutations in X-Linked Charcot-Marie-Tooth Disease

J. Bergoffen,* S. S. Scherer, S. Wang, M. Oronzi Scott, L. J. Bone, D. L. Paul, K. Chen, M. W. Lensch, P. F. Chance, K. H. Fischbeck

X-linked Charcot-Marie-Tooth disease (CMTX) is a form of hereditary neuropathy with demyelination. Recently, this disorder was mapped to chromosome Xq13.1. The gene for the gap junction protein connexin32 is located in the same chromosomal segment, which led to its consideration as a candidate gene for CMTX. With the use of Northern (RNA) blot and immunohistochemistry technique, it was found that connexin32 is normally expressed in myelinated peripheral nerve. Direct sequencing of the connexin32 gene showed seven different mutations in affected persons from eight CMTX families. These findings, a demonstration of inherited defects in a gap junction protein, suggest that connexin32 plays an important role in peripheral nerve.

Charcot-Marie-Tooth disease (CMT) is a pathologically and genetically heterogeneous group of disorders that cause progressive degeneration of peripheral nerves. Affected patients have distal weakness, atrophy, sensory loss, and decreased tendon reflexes. CMT has traditionally been classified by whether the primary pathological defect is degeneration of the myelin (CMT1) or of the axons (CMT2) in the peripheral nerves. Within the demyelinating type of CMT, there is genetic heterogeneity, with similar dominantly inherited disease manifestations produced by genetic defects on chromosomes 17 (CMT1A), 1 (CMT1B), and X (CMTX). Recently, mutations in the chromosome 17– and chromosome 1–linked forms of CMT have been found in the genes for peripheral myelin protein 22 (PMP22) and myelin protein zero (P_0), respectively (*1*, *2*). Here, we report that patients with X-linked CMT have mutations in the gene for the gap junction protein, connexin32 (Cx32, *GJB1*).

Linkage studies and analysis of recombinants were initially used to map CMTX to the proximal long arm of the X chromosome (*3*, *4*) and subsequently to refine the localization to band Xq13 (*5*). Analysis of additional recombinations in CMTX families placed CMTX in a small interval between the markers DXS106 and DXS559 in Xq13.1 (*6*). The gene for Cx32 is known to map to this interval (*7*), and we therefore evaluated it as a candidate gene for CMTX. We performed Southern (DNA) blots of patient DNA to look for rearrangement of the Cx32 gene in CMTX and Northern blots to determine the extent of expression in peripheral nerve RNA. The Southern blots showed no abnormality, but Northern analysis showed expression of the Cx32 gene in peripheral nerve at a level comparable to that in liver and greater than that present in most other tissues (Fig. 1).

Because we found expression of Cx32 in peripheral nerves, we directly sequenced the translated portion of the gene in samples from CMTX patients. We discovered seven variations from the control sequence in eight CMTX families (Figs. 2 and 3): six single-base changes that predict nonconservative amino acid substitutions, and one single-base insertion that shifts the translational reading frame at position 175 and predicts a premature stop signal at position 241. Two families (221 and K1905) from the midwestern United States shared the same mutation at position 139. One other CMTX family (family 63) (*5*) had no detectable mutation in the translated portion of the Cx32 gene.

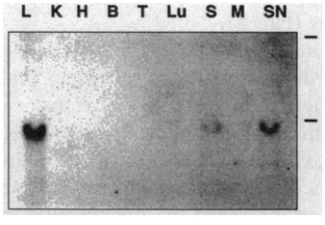

Fig. 1. Northern blot showing expression of Cx32 in peripheral nerve (*19*). The lanes contain 10 μg of total RNA from the following rat tissues; L, liver; K, kidney; H, heart; B, brain; T, thymus; Lu, lung; S, spleen; M, muscle; and SN, sciatic nerve. The hatch marks at right indicate the positions of 28*S* and 18*S* ribosomal RNA, respectively.

J. Bergoffen, Department of Neurology, University of Pennsylvania Medical School and Genetics Division, Children's Hospital of Philadelphia, Philadelphia, PA 19104.
S. S. Scherer, S. Wang, M. Oronzi Scott, L. J. Bone, K. Chen, M. W. Lensch, K. H. Fischbeck, Department of Neurology, University of Pennsylvania Medical School, Philadelphia, PA 19104.
D. L. Paul, Department of Neurobiology, Harvard Medical School, Boston, MA 02115.
P. F. Chance, Department of Neurology, University of Pennsylvania Medical School and Neurology Division, Children's Hospital of Philadelphia, Philadelphia, PA 19104.

*Present address: Genetics Department, Permanente Medical Group, San Jose, CA 95119.

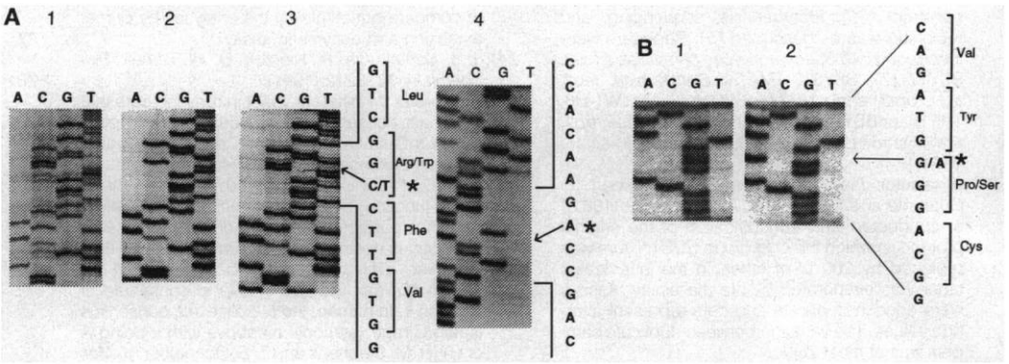

Fig. 2. Sequencing gels showing point mutations in Cx32 in two CMTX families (*20*). (**A**) The mutation at position 142 in family 243. Gels 1 to 3 are sense strands; 1, normal sequence; 2, sequence from an affected male; 3, sequence from a heterozygous female; and 4, antisense strand from an affected male. (**B**) The mutation at position 172 in family 133/K1852 on the antisense strand: 1, normal sequence; 2, sequence from an affected male. The disease samples showed no other variation from the control sequence in the translated portion of the Cx32 gene. Asterisks indicate sites of mutations.

The mutation at position 142 in family 243 results in the loss of an Hpa II restriction endonuclease site, which enabled us to screen for this sequence change by polymerase chain reaction (PCR) amplification and endonuclease digestion (Fig. 4). We found the mutation to segregate with the disease in five affected family members; the screening of eight unaffected family members and 94 unrelated normal individuals (162 chromosomes) did not detect the mutation. The oldest affected member of family 243 had an unaffected sister and nephew who had the same haplotype of close flanking markers (DXS453 and DXS441) but lacked the position 142 mutation, which suggests that the mutation arose de novo in this family. Similarly, the loss of a Bst XI restriction site caused by the mutation at position 175 allowed us to determine the segregation of the mutation with the disease in family 51; the mutation was present in all affected family members studied but absent in unaffected family members and in 52 unrelated normal females (104 chromosomes). The combined maximum lod score for linkage of the Cx32 mutations to CMTX in these families was 11.8 with no recombination (*8*). Prompted by the finding of Cx32 mutations in CMTX patients, we examined the normal distribution of Cx32 protein in rat peripheral nerve by immunohistochemistry. Our results confirmed the presence of Cx32 in myelinated peripheral nerve at the nodes of Ranvier and at Schmidt-Lanterman incisures (Fig. 5).

Connexins are membrane-spanning proteins that assemble to form gap junctions, channels that facilitate the transfer of ions and small molecules from cell to cell. The connexin subunits are incorporated into half channels, or connexons, that interact with their counterparts in neighboring cells to form complete intercellular channels. Twelve different rodent connexin genes have been identified (*9*); expression of the various isoforms varies from tissue to tissue and is developmentally regulated (*10*). In the central nervous system, gap junctions have been identified in neurons, ependymal cells, astrocytes, and oligodendrocytes (*11*). Cx32 is a member of the connexin family that was originally cloned in 1986 (*12, 13*). It is known to be present with other connexins in liver, epithelial cells, and brain (*10*). The temporal appearance of Cx32 mRNA and protein in the brain coincides with postnatal development events such as glial and neuronal maturation, synaptogenesis, myelination, and vascularization (*11*). Gap junctions have not previously been observed in mature mammalian peripheral nerve (*14*).

Cx32 has two extracellular loops, four transmembrane segments, and three cytoplasmic domains (*10*) (Fig. 3). The amino acid sequence is well conserved across species, particularly in the extracellular and transmembrane domains. The amino acid residues altered by the CMTX point mutations are generally conserved in vertebrates and are located in portions of the protein that are believed to be functionally important. If, as suggested (*15*), the third transmembrane domain forms a part of the gap junction pore, then the changes at positions 139 and 142 might impair or block channel formation. The proline at position 172 is adjacent to a highly conserved cysteine at position 173, which may form a disulfide bond important to gap junction structure. Change of the cysteine to serine at position 173 leads to a loss of channel formation in oocytes (*16*); a change at position 172 may have a similar deleterious effect. The frame-shifting mutation at position 175 would abolish another highly conserved cysteine at position 179 as well as the entire fourth transmembrane domain

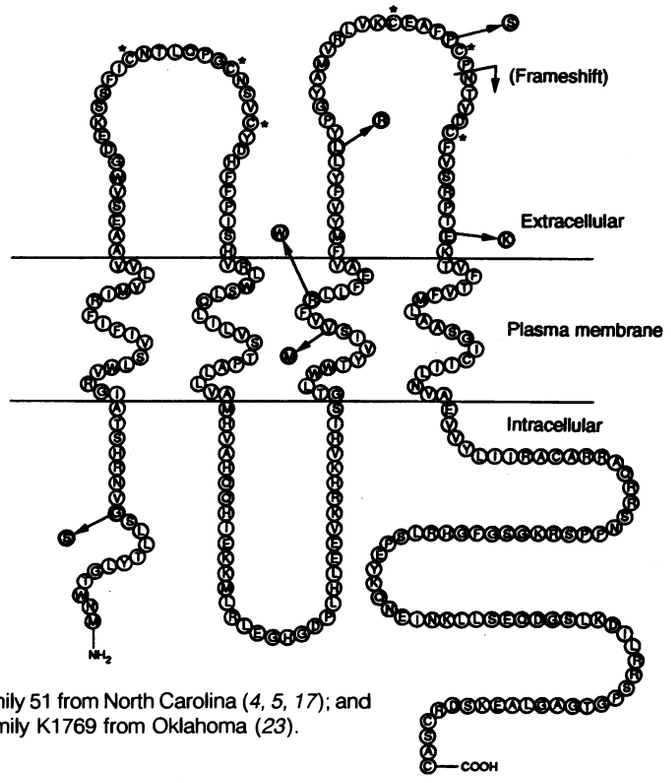

Fig. 3. Diagram of Cx32, showing transmembrane orientation, conserved cysteine residues (asterisks), and locations of the CMTX mutations (arrows) (*21*). The Cx32 structure is based on (*10, 16*). The indicated mutations are as follows: G12S, GGC → AGC in family 58 from Belgium (*4, 22*); V139M, GTG → ATG in families 221 and K1905 from South Dakota and Michigan, respectively [discussed in this paper and (*23*)]; R142W, CGG → TGG in family 243 from Pennsylvania (discussed in this paper); L156R, CTC → CGC in family 251 from Pennsylvania (discussed in this paper); P172S, CCC → TCC in family 133/K1852 from North Carolina (*5, 23*); 175 frameshift, A insertion in family 51 from North Carolina (*4, 5, 17*); and E186K, GAG → AAG in family K1769 from Oklahoma (*23*).

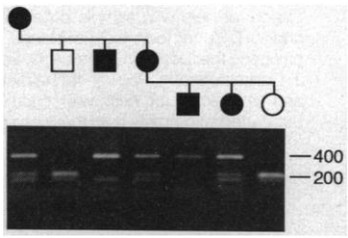

Fig. 4. Segregation of the position 142 mutation in family 243, as demonstrated by Hpa II digestion. Genotypes were determined by PCR amplification of a fragment of the Cx32 translated region (*20*) and subsequent digestion with Hpa II. Each reaction was electrophoresed in a 1% agarose gel with ethidium bromide for visualization. The top diagram shows the family pedigree with affected females (filled circles), affected males (filled squares), unaffected females (open circles), and unaffected males (open squares). Disease status was determined by the presence of distal extremity weakness, atrophy, sensory loss, and loss of tendon reflexes on neurological examination. In the gel below, all five affected individuals show a ~400-bp fragment uncut by Hpa II, whereas unaffected individuals and heterozygous females demonstrate a ~200-bp band that represents a doublet cut with Hpa II.

and the COOH-terminal intracellular domain. The predicted effects of these sequence variations on important, highly conserved portions of the protein suggest that they are causative mutations rather than coincidental polymorphisms.

Sequence variation was not detected in the translated portion of the Cx32 gene in one of nine CMTX families studied. It remains possible that a mutation is present in the untranslated or regulatory portion of this gene in this pedigree. Alternatively, the disease mechanism in this family could involve a dosage effect, as has been reported in CMT1A (*1*).

Although Cx32 is present in other tissues, such as liver and brain, the manifestations of CMTX appear to be limited to peripheral nerves. This may mean that other connexins can substitute for the function of Cx32 elsewhere but not in peripheral nerves. Nevertheless, the association of Cx32 mutations with a peripheral nerve disease suggests that Cx32 is particularly important to peripheral nerve structure and function. The immunohistochemical distribution of Cx32 protein at the nodes of Ranvier and Schmidt-Lanterman incisures suggests that Cx32 may form intracellular gap junctions that connect the folds of Schwann cell cytoplasm. This would allow transfer of ions, nutrients, and other small molecules around and across the compact myelin to the innermost myelin layers, perhaps indirectly providing sustenance to the axon as well. This would explain the combination of myelin disruption and axonal degeneration that occurs with Cx32 mutations in CMTX (*17, 18*).

The connexin family of proteins has been well studied in a variety of systems, including detailed study of the effects of site-directed mutagenesis on channel formation in vitro. Our findings show naturally occurring connexin mutations and provide insight into the physiological role of connexins and gap junctions in vivo.

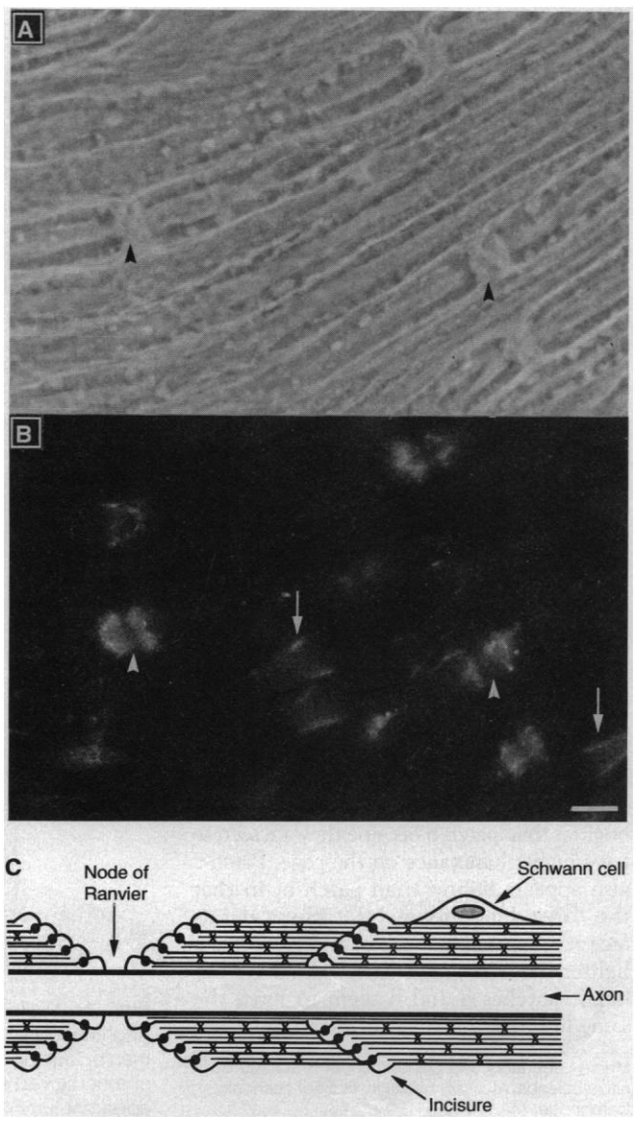

Fig. 5. Immunofluorescent localization of Cx32 in rat sciatic nerve (*24*). The sections were examined by phase contrast (**A**) and immunofluorescence (**B**). Intense, finely granular staining is observed adjacent to the nodes of Ranvier (arrowheads). Signal is also detected in the Schmidt-Lanterman incisures (arrows), which are not well resolved in the phase-contrast micrograph. No staining above background was observed in axons or in compact myelin. Scale bar: 10 μm. (**C**) The difference in distribution of Cx32 (circles) compared to PMP22 and P_0 (marked with X's), the products of the other genes that have been implicated in inherited demyelinating neuropathy (CMT1).

REFERENCES AND NOTES

1. P. I. Patel *et al.*, *Nature Genet.* **1**, 159 (1992); L. J. Valentijn *et al.*, *ibid.*, p. 166; V. Timmerman *et al.*, *ibid.*, p. 171; N. Matsunami *et al.*, *ibid.*, p. 176; L. J. Valentijn *et al.*, *ibid.* **2**, 288 (1992); B. B. Roa *et al.*, *N. Engl. J. Med.* **329**, 96 (1993).
2. K. Hayasaka *et al.*, *Nature Genet.* **5**, 31 (1993); T. Kulkens *et al.*, *ibid.*, p. 35.
3. A. Gal *et al.*, *Hum. Genet.* **70**, 38 (1985); J. Beckett, N. E. Holden, B. N. Simpson, B. N. White, P. M. MacLeod, *J. Neurogenet.* **3**, 225 (1986).
4. K. H. Fischbeck *et al.*, *Ann. Neurol.* **20**, 527 (1986).
5. J. Bergoffen *et al.*, *Am. J. Hum. Genet.* **52**, 312 (1993).
6. J. Bergoffen *et al.*, *Am. J. Hum. Genet.* **53** (suppl.), 977 (abstr.) (1993).
7. I. A. Corcos *et al.*, *Genomics* **13**, 479 (1992); E. Raimondi *et al.*, *Cytogenet. Cell Genet.* **60**, 210 (1992).
8. The lod score was determined with the LIPED computer program [J. Ott, *Am. J. Hum. Genet.* **26**, 588 (1974)].
9. R. Dermietzel and D. C. Spray, *Trends Neurosci.* **16**, 186 (1993).
10. M. V. L. Bennett *et al.*, *Neuron* **6**, 305 (1991).
11. D. J. Belliveau, G. M. Kidder, C. C. G. Naus, *Dev. Genet.* **12**, 308 (1991).
12. D. L. Paul, *J. Cell Biol.* **103**, 123 (1986).
13. N. Kumar and N. B. Gilula, *ibid.*, p. 767.
14. G. Gabriel, P. K. Thomas, R. H. M. King, C. Stolinski, A. S. Breathnach, *Acta Neuropathol.* **72**, 62 (1986); K. Akert, C. Sandri, E. R. Weibel, K. Peper, H. Moor, *Cell Tissue Res.* **165**, 281 (1976).
15. L. C. Milks, N. Kumar, R. Houghton, N. Unwin, N. B. Gilula, *EMBO J.* **7**, 2967 (1988).
16. G. Dahl, R. Werner, E. Levine, C. Rabadan-Diehl, *Biophys. J.* **62**, 172 (1992).
17. M. P. Rozear *et al.*, *Neurology* **37**, 1460 (1987).
18. A. F. Hahn, W. F. Brown, W. J. Koopman, T. E. Feasby, *Brain* **113**, 1511 (1990).
19. The technique for Northern blot analysis was as described [B. Friedman *et al.*, *Neuron* **9**, 295 (1992)]. Total RNA was isolated from the indicated rat tissues as described [J. M. Chirgwin, A. E. Pryzbyla, R. J. MacDonald, R. J. Rutter, *Biochemistry* **18**, 5294 (1979)]. The RNA was separated on a

1% agarose gel, transferred to a nylon membrane overnight in 6× saline sodium citrate (SSC), and hybridized overnight with a radiolabeled complementary DNA probe for rat Cx32 (*7*). The blot was washed at a final stringency of 0.2× SSC for 30 min at 65°C and exposed to x-ray film with an intensifying screen for 5 days at −80°C. Approximately equal loading of samples in each lane was assured by comparison of the intensity of ethidium-stained ribosomal RNA bands in the gel and by rehybridization of the membrane with a complementary DNA probe for the housekeeping gene glyceraldehyde-3-phosphate dehydrogenase.

20. Blood was obtained from CMTX patients by informed consent, and genomic DNA was isolated from venous blood by standard methods (*4*). The connexin32 coding region was amplified with PCR with various primer sets spanning this region. The segment including bases 54 to 359 (*13*) was amplified with the primer set 5′-TGAGGCAGGATGAACTGGACAGGT-3′ (bases 54 to 77) and 5′-TTGCTGGTGAGCCACGTGCATGGC-3′ (bases 336 to 359), and the segment including bases 273 to 938 was amplified with the primer set 5′-ATCTCCCATGTGCGGCTGTGGTCC-3′ (bases 273 to 296) and 5′-TGGCAGGTTGCCTGGTATGT-3′ (bases 919 to 938). Twelve picomoles of each primer set was used in a reaction volume of 100 μl with 100 to 200 ng of genomic DNA as a template. PCR conditions for the first primer set were 94°C for 7 min; 94°C for 30 s, 65°C for 30 s, and 72°C for 30 s (35 cycles); and 72°C for 10 min. Conditions for the second primer set were 94°C for 5 min; 94°C for 1 min, 63°C for 1 min, and 72°C for 1 min (35 cycles); and 72°C for 10 min. Amplified products were purified with the Gene Clean protocol (BIO 101) and subsequently used as templates for sequencing at 20 to 50 ng per reaction. The primers listed above were used for sequencing; in addition, the following primers were used for bases 273 to 704 and 635 to 933, respectively: 5′-GATGATGAGGTACACCACCT-3′ (bases 685 to 704) and 5′-CGTCTTCATGCTAGCTGCCTCTGG-3′ (bases 635 to 658). The sequencing reactions were set up according to manufacturer's recommendations with the Sequenase Version 2.0 kit (U.S. Biomedicals) with minor modifications (10 pmol of primer per reaction; 50°C termination for 5 min).
21. Abbreviations for the amino acid residues are: A, Ala; C, Cys; D, Asp; E, Glu; F, Phe; G, Gly; H, His; I, Ile; K, Lys; L, Leu; M, Met; N, Asn; P, Pro; Q, Gln; R, Arg; S, Ser; T, Thr; V, Val; W, Trp; and Y, Tyr. Mutations are indicated with the single-letter code; thus, $Gly^{12} \rightarrow Ser$ is given by G12S.
22. J. P. Fryns and H. Van Den Berghe, *Hum. Genet.* **55**, 413 (1980).
23. P. R. Fain, D. S. Barker, P. F. Chance, *Am. J. Hum. Genet.*, in press.
24. Adult rat sciatic nerve was fixed in 1.6% formaldehyde in Hank's buffered salts (Gibco) for 1 hour at room temperature. The tissue was then transferred to tris-buffered saline (TBS) and incubated for 2 hours at 4°C, followed by incubation in 0.5 M sucrose overnight for cryoprotection. Samples were quick-frozen in OCT (Miles Scientific, Elkhart, IN) with liquid freon, and 10- to 12-μm cryosections were collected. The sections were mounted on slides, air dried, then incubated in acetone for 5 min at room temperature. After rehydration in TBS for 5 min, the sections were blocked for 15 min in 2% fish skin gelatin (Sigma), 1% normal goat serum, and 0.25% Triton X-100 in TBS (blocking solution), then incubated with a 1/1000 dilution of Cx32 antiserum (anti-98/124) [D. A. Goodenough, D. L. Paul, L. Jesiatis, *J. Cell Biol.* **107**, 1817 (1988)] in blocking solution for 1 hour at room temperature. The sections were washed twice in 50 ml of TBS with 0.25% Triton X-100 and once with TBS, then incubated with 1/500 rhodamine-conjugated goat antibody to rabbit (Pierce) in blocking buffer. The sections were washed and mounted for immunofluorescence microscopy as described (*12*).

25. We thank the families studied for their cooperation; J. P. Fryns, M. Rozear, M. Pericak-Vance, and J. Stajich for help with sample collection; C. Litrenta and Y.-T. Yu for technical assistance; I. Corcos for providing the Cx32 cDNA probe; C. Lo, J. Kamholz, J. Garbern, and H. Paulson for helpful discussions; and V. Valmiki for help with figure preparation. Supported with grants from the Muscular Dystrophy Association, the March of Dimes Birth Defects Foundation, and NIH (NS08075, NS01565, GM37751, and NS30804). J.B. was supported by a fellowship from The Charles A. Dana Foundation.

25 August 1993; accepted 12 November 1993

Perceptual Organization and the Judgment of Brightness

Edward H. Adelson

The perceived brightness of a gray patch depends on the surrounding context. For example, a medium-gray patch appears darker when placed on a bright background and brighter when placed on a dark background. Models to explain these effects are usually based on simple low-level mechanisms. A new set of brightness illusions cannot be explained by such models. In these illusions, the brightness percept is strongly influenced by the perceptual organization of the stimuli. Simple modifications of the stimuli that should have little effect on low-level mechanisms greatly alter the strength of the illusion. These effects may be ascribed to more complex mechanisms occurring later in the visual system.

A gray patch appears brighter when viewed against a dark background and darker when viewed against a bright background. This effect, known as "simultaneous contrast," is one of many brightness effects that are commonly attributed to simple visual processes, such as the lateral inhibition that occurs in the retina (*1*), whereby cells in one region inhibit cells in adjacent regions. Another class of models, known as retinex models, have been offered to explain the perception of surface colors in terms of the propagation of information about local luminance changes (*2*). Both kinds of model are founded on low-level processes that involve simple interactions between neighboring neurons. The outputs of such models should be unaffected by a display's higher-level perceptual properties, such as the perceived depth and form. But we have found that a change in perceptual interpretation can have a profound effect on the judgment of brightness.

Following the customary terminology (*3*), lightness refers to the apparent reflectance of a surface in a scene, whereas brightness refers to the apparent luminance of a patch in the image itself. That is, an observer in a brightness experiment is asked to judge the shade of ink on the page but not to make any inferences about the surfaces of the objects portrayed. In Fig. 1, patches a and c are obviously brighter than patch b because they are seen to have higher luminance on the page. Patch c also appears lighter than patch b, in that the three-dimensional (3D) physical surface represented by c seems to be painted a lighter shade of gray than b. On the other hand, patches a and b seem to have the same lightness, as they appear to represent surfaces painted the same shade.

Lightness judgments can be influenced by high-level perceptual factors (*4*, *5*). Figure 1 makes the point with a simple image: The geometry leads to a 3D interpretation that causes patch b to match patch a in apparent reflectance (lightness) but not to match patch c, which has the same luminance as patch a. Lightness can also be affected by the perception of surface curvature (*6*). These various lightness phenomena cannot be explained by low-level models. Because an observer in a lightness experiment is judging properties of the objects portrayed, rather than merely estimating the brightness of the ink on the page, one might not be surprised to find that low-level mechanisms fail to explain the results.

In our experiments, we used simple stimuli displayed on a computer screen and used the more "sensory" brightness judgment

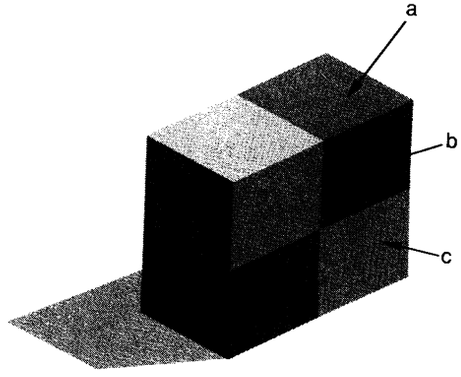

Fig. 1. Distinction between lightness and brightness. Patch c is both lighter and brighter than b. Lightness refers to apparent reflectance of a perceived surface; brightness refers to the apparent luminance of a patch in an image.

Media Laboratory and Department of Brain and Cognitive Science, Massachusetts Institute of Technology, Cambridge, MA 02139.